On the Estimation of the Radial Distance of a Moving Person in Indoor Environments from the Demodulated Response of LFMCW Radars

Rym Hicheri, Muhammad Muaaz, Nurilla Avazov, and Matthias Pätzold
Faculty of Engineering and Science, University of Agder, P.O. Box 509, 4898 Grimstad, Norway
E-mails: {rym.hicheri, muhammad.muaaz, nurilla.avazov, matthias.paetzold}@uia.no

***Abstract*—This paper deals with the estimation of the time-variant (TV) radial distance of a moving person in an indoor environment. The TV radial distance is obtained from the amplitude of the demodulated TV radar response. For simplicity, the body of a person is modelled by a single point scatterer. We start by determining the TV path delay caused by the motion of the person. Then, the TV radial distance is deduced from the estimated TV path delay. To confirm the validity of the estimation method, we conduct real-world measurements. In this regard, two experiments are carried out for which the radio-frequency (RF) data is collected using the Ancortek SDR-KIT 2400T2R4 radar system operating at 24 GHz. In the first experiment, we consider a swinging pendulum acting as a single moving point scatterer. We compare the estimated TV radial distance of the pendulum with the corresponding theoretical expression that provides the ground truth information. For this experiment, the good match between the measured and analytical results demonstrates the proof of concept. In the second experiment, we consider a walking person acting as a single moving for which we can accurately compute the total travelled distance. The findings confirm the validity of the estimation method.**

***Index Terms*—Radial distance estimation, localization techniques, moving person, indoor environments, TV demodulated radar response, LFMCW radars.**

I. Introduction

Linear frequency modulated continuous wave (LFMCW)-based millimeter-wave (mmWave) radar sensors have attracted great interest in recent years for both indoor and outdoor applications [1], [2]. This is motivated by their high range resolution, low power consumption, and simple structure compared to ultrasound or infrared sensors [3]–[5].

One of the many applications of LFMCW radars is to estimate the range of a moving target. Traditionally, the target's time-variant (TV) radial distance information is extracted from the range profile or the range-Doppler profile computed from the received radio-frequency (RF) LFMCW signals [6], [7]. For example, the authors of [8] investigated the range in the context of multiple-input multiple-output video synthetic radar with beat frequency division FMCW in unmanned aerial vehicle environments. This is performed by employing frequency-estimation algorithms to compute the area of the beat signal from which the target's TV radial distance is obtained. These algorithms extract the range information from the amplitude or phase of the range profile. The Jacobsen algorithm [9] is an example of a range estimation method, which leverages the information contained in the amplitude of the range profile. On the other hand, phase-based methods are best exemplified by the Quinn algorithm [10]. Later, the hybrid J-Quinn algorithm, which combines amplitude and phase information, was proposed in [11].

Range-based techniques for human activity monitoring in indoor environments were widely investigated. In [12], the impact of human gait on radar signals was analyzed using time-frequency methods. The authors of [13] proposed a simulation-based facet model to investigate inverse synthetic aperture radar images and radar back-scattering of moving persons. Feature extraction and human activity classification using LFMCW radar systems in indoor spaces were the topic of [14]. Range tracking using mmWave LFMCW radars was also applied to non-contact monitoring of vital signs, focusing mainly on heartbeats and respiratory patterns [15]–[18].

All the above mentioned studies rely on the range profile or range-Doppler profile to determine the TV range or radial distance of a moving target. To the best of the authors' knowledge, the estimation of the TV radial distance of a moving person from the TV channel transfer function (TVCTF) or the TV demodulated radar response [19] of indoor non-stationary radio channels using LFMCW radars is unknown. Hence, this motivates us to propose a method to extract the TV radial distance of a moving person by using the TV demodulated radar response.

In this paper, we estimate the TV radial distance (range) of a moving person (target) in an indoor environment, which is equipped with an LFMCW radar system. The person is modelled by a single point scatterer representing the centre of mass (CoM) of the body. The TV radial distance of a moving person is estimated from the amplitude of the demodulated radar response, which is related to the received beat signal. This method is validated by performing two real-world measurement campaigns in a laboratory-like room. We employ the Ancortek SDR-KIT 2400T2R4 device, which is a LFMCW radar system operating at 24 GHz. We configure this device as a single-input single-output (SISO) communication system, where the antennas are collocated. First, a pendulum experiment is conducted, for which the ground truth (exact) TV trajectory is known from the pendulum's equation of motion [20]. We compared the estimated TV radial distance with the corresponding exact quantity. A good match is

978-1-6654-2854-5/21/$31.00 ©2021 IEEE

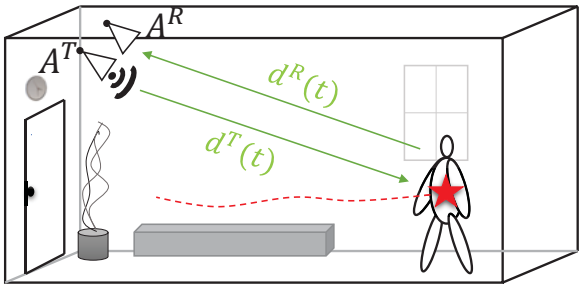

Fig. 1. Description of the indoor scenario with a single moving person (scatterer).

observed between measured and theoretical results. Based on this validated method, we conducted a real-life experiment, where a person performed a walking activity. The total walked distance is then estimated from the demodulated radar response using our proposed method

The rest of the paper is organized as follows. A description of the indoor scenario is presented in Section II. The algorithm to extract the TV radial distance of the target from the TV demodulated radar response is presented in Section III. The validation pf the proposed algorithm using measured RF data is reported in Section IV. Finally, the conclusion is drawn in Section V.

II. Scenario Description

The indoor scenario investigated in this paper is illustrated in Fig. 1. As can be seen, we consider an indoor environment equipped with an LFMCW radar system, which is comprised of a fixed transmit antenna A^T and a fixed receive antenna A^R. The antennas A^T and A^R are located at the positions (x^T, y^T, z^T) and (x^R, y^R, z^R), respectively. As shown in Fig. 1, there is a single moving person, which is modelled by a single point scatterer S^M. The moving point scatterer S^M represents the CoM of the person's body. The scatterer S^M has TV positions $x(t)$, $y(t)$, and $z(t)$. The TV Euclidean distance between the transmit antenna A^T and the scatterer S^M is denoted by $d^T(t)$, which can be computed as

$$d^T(t) = \sqrt{(x(t) - x^T) + (y(t) - y^T) + (z(t) - z^T)}. \quad (1)$$

Similarly, the TV distance $d^R(t)$ represents the Euclidean distance between the scatterer S^M and the receive antenna A^R, which can be expressed as

$$d^R(t) = \sqrt{(x(t) - x^R) + (y(t) - y^R) + (z(t) - z^R)}. \quad (2)$$

Finally, single-bounce scattering is assumed when modelling the moving point scatterer S^M.

In the following, we assume that the transmit and receive antennas are collocated. In this case, we denote by $r(t) = d^T(t) = d^R(t)$ the TV radial distance of the moving person (point scatterer S^M). The radial distance refers to the TV Euclidean distance between the moving scatterer S^M and the transmit/receive antenna.

III. Non-Stationary Channel Model for LFMCW Radars

LFMCW radar systems transmit a continuous chirp of duration T and bandwidth B. In the presence of a moving scatterer S^M (see Section II), the received signal can be seen as a scaled and delayed version of the transmitted signal in the slow-time (resp. frequency) domain. Then, a dechirping procedure is applied to the received LFMCW signal to retrieve the so-called low-pass filtered beat signal [15, Eq. (4)]. As is discussed in [19], for indoor scenarios, the TVCTF $H(t, f')$ corresponding to the indoor propagation scenario described in Section II can be obtained as the complex conjugate of the beat signal of LFMCW radar systems as

$$H(t, f') = c(t) \exp\left(-j\left(2\pi(f' + f_c)\tau'(t)\right)\right) \quad (3)$$

where f_c is the centre carrier frequency. The TVCTF $H(t, f')$ describes the channel in the time-frequency domain, in which t refers to the observation time (slow-time) and $f' \in [-B/2, B/2]$ stands for the instantaneous frequency of the LFMCW radar (also known as the subcarrier frequency).

In (3), the complex path gain $c(t)$ depends on the antenna gains, path loss exponent, low-noise amplifiers, etc. According to the free-space path loss model [21, pp. 49], the path gain $c(t)$ can be expressed as $c(t) = ad(t)^{-\gamma/2} \exp(j\theta)$, where a is the radar cross-section, $d(t)$ is the attenuation distance, and γ is the path loss exponent. When the wave propagation is taking place in an indoor area, the value of γ is typically between 1.6 and 1.8. Here, θ is the initial phase of the channel and takes into consideration the phase shift introduced by the propagation environment. The phase θ can be modelled by a random variable, which follows the uniform distribution over the interval $(-\pi, \pi)$. Moreover, the TV path delay introduced by the moving scatterer S^M is expressed in terms of the TV distances $d^T(t)$ and $d^R(t)$ as $\tau'(t) = [d^T(t) + d^R(t)]/c_0$, where c_0 refers to the speed of light. For the specific scenario, where the transmit and receive antennas are collocated, the TV radial distance $r(t)$ can be obtained as

$$r(t) = d^T(t) = d^R(t) = c_0\tau'(t)/2. \quad (4)$$

Traditionally, fading channels can also be characterized in the time-delay domain by means of the channel impulse response [22, Section 3.1]. For the case of LFMCW radars, the equivalent quantity is referred to as the demodulated radar response, which is denoted by $h(t, \tau')$ and can be obtained by performing an inverse fast Fourier transform (IFFT) w.r.t. instantaneous frequencies f' over each period $[-B/2, B/2]$ of the TVCTF $H(t, f')$ in (3) as

$$\begin{aligned} h(t, \tau') &= \int_{-B/2}^{B/2} H(t, f') \exp\left(j2\pi f'\tau'\right) df' \\ &= B\, c(t)\, \mathrm{sinc}\left[B\left(\tau' - \tau'(t)\right)\right] \exp\left(-j2\pi f_c \tau'(t)\right) \end{aligned} \quad (5)$$

in which $\mathrm{sinc}(\cdot)$ refers to the normalized sinc function, which is defined as $\mathrm{sinc}(x) = \sin(x)/x$ for $x \neq 0$. Here, it is assumed

that the TV path gain $c(t)$ and TV path delay $\tau'(t)$ remain constant for the chirp duration T.

IV. Extraction of the TV Radial Distance of the Moving Person

In this section, we present the algorithm adopted to estimate the TV path delay $\tau'(t)$ from which the TV radial distance $r(t)$ is deduced. As can be observed from (5), the TV path delay $\tau'(t)$ can be directly extracted as the maximum value of the absolute value of the TV demodulated radar response $h(t,\tau')$. Thus, the TV path delay $\tau'(t)$ at each time instant t is obtained as

$$\tau'(t) = \max_{\tau'} |h(t,\tau')|. \tag{6}$$

Then, the TV radial distance $r(t)$ of the moving person is determined as $r(t) = c_0\tau'(t)/2$.

After demodulation, the samples of the received LFMCW signal are acquired by an analog-to-digital converter (ADC). In this regard, the ADC samples are obtained as a vector of length $P \times Q$, where P is the number of bins of slow-time instances t_p $(p = 1, 2, \ldots, P)$ and Q is the number of frequency (linearly proportional to fast-time) instances f'_q $(q = 1, 2, \ldots, Q)$ for a single chirp. Then, the ADC samples are dechirped and reshaped to obtain the beat signal $\mathbf{B}[p,q]$ for $p = 1, 2, \ldots, P$ and $q = 1, 2, \ldots, Q$. The beat signal $\mathbf{B}[p,q]$ is a matrix of dimension $P \times Q$. Next, the channel matrix, denoted by $\mathbf{H}[p,q]$, is deduced from the beat signal $\mathbf{B}[p,q]$ as $\mathbf{H}[p,q] = \mathbf{B}^*[p,q]$. Here, $\mathbf{H}[p,q] = H(t_p, f'_q)$.

Afterwards, the TV radial distance $r(t_p)$ at the time instant t_p is estimated according to the following steps:

1) Perform an N_{IFFT}-points IFFT over each line (slow-time bin) of the matrix $\mathbf{H}[p,q]$. The resulting TV demodulated radar response is denoted by $\mathbf{S}[p,n]$, which contains the values of $h(t_p, \tau'_n)$ for $n = 1, 2, \ldots, N_{\text{IFFT}}$. Here, τ'_n corresponds to the nth delay instance, where $\tau'_0 = 0$ and $\tau'_{N_{\text{IFFT}}} = \tau'_{\max}$. The value of $\tau'_{\max}$ depends on the IFFT parameters, the unambiguous range of the radar, and the filtering parameters [16], [23].
2) Choose the pth slow-time bin (corresponding to the pth row of the matrix $\mathbf{S}[p,n]$). Introduce a vector $\mathbf{s}_p[n] = \mathbf{S}[p,n]$, for $n = 1, 2, \ldots, N_{\text{IFFT}}$.
3) Find the value $\hat{n}$ corresponding to the index of the element with the largest absolute value in $|\mathbf{s}_p[n]|$ $(n = 1, 2, \ldots, N_{\text{IFFT}})$. Then, the estimated value of the TV path delay at the pth slow-time bin is obtained as $\mathbf{s}[p] = \tau'(t_p) = \tau'_{\hat{n}}$.
4) Finally, the TV radial distance $\mathbf{r}[p]$ at the pth slow-time bin is deduced as $\mathbf{r}[p] = r(t_p) = \mathbf{s}[p] \times c_0/2$.

In addition, two points must be addressed before describing the validation using measurements data. First, it has been assumed that the moving person (modelled by the point scatterer S^M) is located at the same TV radial distance $r(t)$ for the chirp duration T. Secondly, high-pass filtering is applied to reduce the impact of ambient noise. Since the fixed scatterers (modelling the fixed objects in the room) do not experience any Doppler shift, the high-pass filter will also mitigate their contribution to the overall propagation phenomenon.

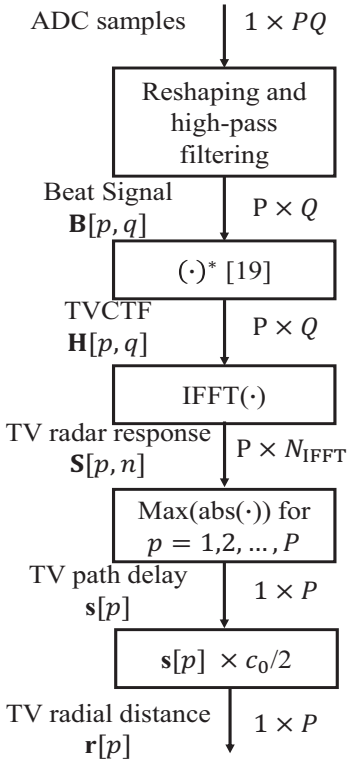

Fig. 2. Estimation of the vector $\mathbf{r}[p]$ containing the samples of the TV radial distance $\mathbf{r}[p] = r(t_p)$.

A summary of the signal processing steps required for the estimation of the TV radial distance $r(t)$ of a moving person in indoor areas from the TV demodulated response of LFMCW radar systems is presented in Fig. 2.

V. Measurement and Numerical Results

In this section, measurements are carried out to assess the performance of the estimation method. This can be achieved by comparing the exact (ground truth) TV radial distance of the moving scatterer S^M with the TV radial distance estimated from the measured TV demodulated radar response. To do so, the knowledge of the exact TV radial distance is required. To the best of the authors' knowledge, the studies on channel models describing human activities are limited. For this reason, we consider two different real-world experiments in the following. First, to provide a comprehensive proof of concept, we consider a pendulum experiment, for which the exact TV trajectories $x(t)$, $y(t)$, and $z(t)$ of the pendulum are known [20]. In the second experiment, a single person is performing a walking activity. Our proposed algorithm is applied to estimate the total distance walked by this person during the observation time.

Both experiments are performed using the same setting. We use the Ancortek SDR-KIT 2400T2R4 system, which is a LFMCW radar operating in the 24 GHz frequency band.

Fig. 3. Measurement setup.

As can be seen in Fig 3, the transmit antenna A^T and the receive antenna A^R are mounted on two tripods at a height of $h_A = 1.1$ m. The centre of the room is assumed to be the initial position of the CoM of the pendulum. The antennas A^T and A^R are co-located at the position $(-1.1, 0, 1.08)$. They are connected to the radar kit by RF cables of length $l_c = 1$ m. The chirp duration T and bandwidth B are set to 0.001 s and 500 MHz, respectively. The centre carrier frequency f_c is equal to 24.250 GHz. In the following, a mean removal/subtraction was applied to remove the impact of the fixed scatterers (objects). Furthermore, high-pass filtering was performed to mitigate the impact of ambient noise, which improves the accuracy of the estimation results. Here, we use an equiripple filter with a stop-band frequency of 0.5 rad/s, a pass-band frequency of 50 rad/s, a stop-band attenuation of 10 dB, and a pass-band ripple of 1 dB. Finally, to compute the demodulated TV radar response, we apply an IFFT on the TVCTF of the measured RF channel w.r.t. the subcarrier frequencies f'_q. The number of points of the IFFT was set to $N_{\text{IFFT}} = 1024$.

A summary of the measurement setting parameters for the experiments is presented in Table I.

TABLE I
MEASUREMENT SETTING PARAMETERS.

Name	Symbol	Value
Centre carrier frequency	f_c	24.125 GHz
Bandwidth	B	500 MHz
Chirp duration	T	0.001 s
Observation time for Experiment 1	T_1	10 s
Observation time for Experiment 2	T_2	10 s
Length of the rope	L	1.52 m
Position of antenna A^T	(x_T, y_T, z_T)	$(-1.1, 0, 1.1)$ m
Position of antenna A^R	(x_R, y_R, z_R)	$(-1.1, 0, 1.1)$ m
Radar cable length	l_c	1 m
Tripod height	h_A	1.1 m
Initial position of the ball	(x_0, y_0, z_0)	$(0, 0, 0)$ m
Maximum displacement of the ball	$x_{\max}$	0.65 m
Height of the person	h_p	1.71 m
Number of points of the IFFT	N_{IFFT}	1024

A. Experiment 1: Swinging pendulum

In Fig. 4, we present the setting for the pendulum experiment (single point scatterer). As can be seen, a medicine ball weighting 3 kg plays the role of the pendulum. Here, the scatterer S^M models the CoM of the ball. The exact TV trajectories $x(t)$, $y(t)$, and $z(t)$ of S^M are determined according to [20], [24] as

$$x(t) = L \sin\left[\arcsin\left(\frac{x_{\max}}{L}\right)\cos\left(\frac{g}{L}t\right)\right] \quad (7)$$

$$y(t) = 0 \quad (8)$$

$$z(t) = L\left[1 - \cos\left[\arcsin\left(\frac{x(t)}{L}\right)\right]\right] \quad (9)$$

where L is the length of the rope, $x_{\max}$ is the maximum displacement along the x-axis, and g is the acceleration of gravity. In Experiment 1, the ball is attached to the ceiling by a non-elastic rope of a length L equal to 1.52 m (see Fig. 4(a)). The pendulum is swinging in the xz-plane (backward-forward motion) with a maximum displacement $x_{\max}$ of 0.65 m (see Fig. 4(b)).

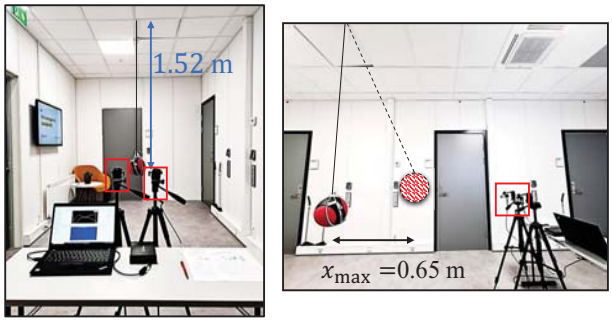

(a) (b)

Fig. 4. View of Experiment 1 from the front (a) and the side (b).

In Fig. 5, we present the demodulated TV radar response $h_c(t, \tau')$. The estimated TV radial distance $r(t)$ of the scatterer S^M is depicted in Fig. 6. The corresponding exact quantities, which are computed using the ground truth TV positions of S^M (see Eqs. (7)–(9)), are also presented to evaluate the accuracy of the estimation method. As can be observed, there is a good match between the estimated radial distance and the exact radial distance. This confirms the validity of the proposed estimation method. This experiment demonstrates the proof of concept.

B. Experiment 2: Walking person

As depicted in Fig. 7, the second experiment considers a single moving person in an laboratory-like environment. The

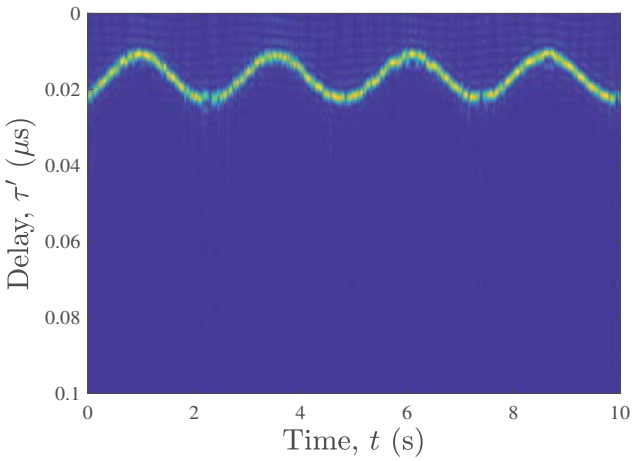

Fig. 5. TV demodulated LFMCW radar response $h_c(t, \tau')$ obtained from the measurements of Experiment 1.

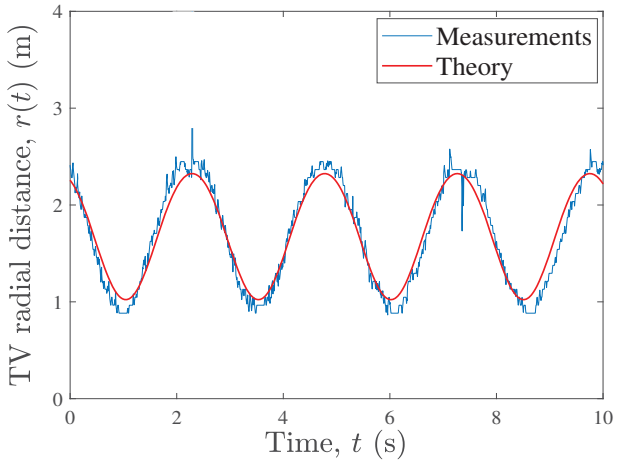

Fig. 6. Comparison of the estimated TV radial distance $r(t)$ with the corresponding theoretical results.

person is male and of height $h_p = 1.71$ m. The person is initially located in front of the LFMCW radar system. At the beginning of Experiment 2, the person is standing still for approximately 2.5 s. Then, the person starts walking away from the radar system following a straight line. The total distance walked by the person is measured using a measuring tape to be 12 m. As the antennas are located at a height equal to h_A =1.1 m, they are directed to capture the movement of the lower back area. Although different body segments in the abdomen area contribute to the propagation phenomenon, their contribution can be merged. Thus, the assumption that the scatterer S^M represents the CoM of the person is valid.

The TV demodulated radar response $h(t, \tau')$, which was obtained from the measurement data of Experiment 2, is presented in Fig. 8. Here, a single component (line) is observed in the TV demodulated radar response $h(t, \tau')$. This corroborates the assumption that the person can be modelled in our experimental setting by a single point scatterer. As can be

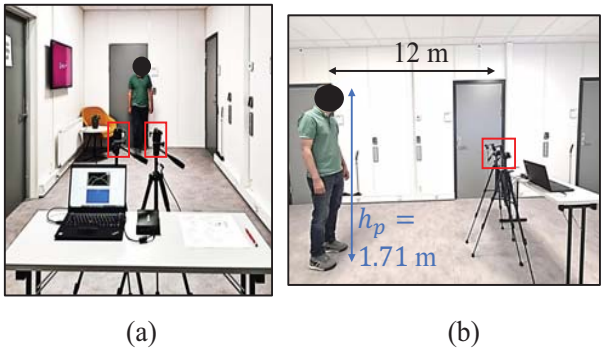

Fig. 7. View of Experiment 2 from the front (a) and the side (b).

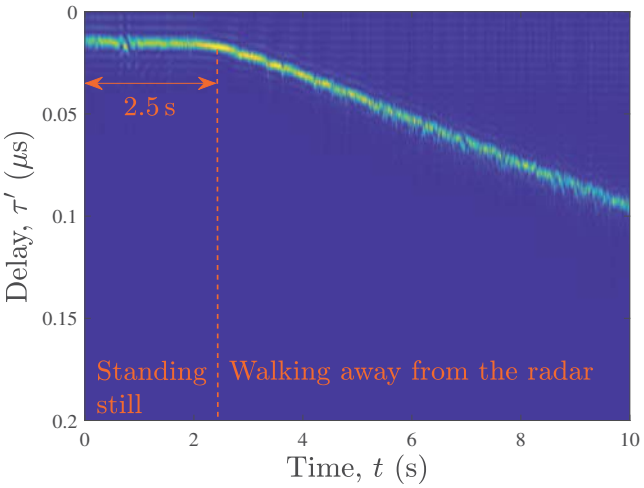

Fig. 8. TV demodulated LFMCW radar response $h(t, \tau')$ obtained from the measurements of Experiment 2.

observed in Fig. 8, the TV demodulated radar response $h(t, \tau')$ can be divided into two parts. In the first part, which lasts about 2.5 s, the TV path delay $\tau'(t)$ introduced by the person is constant. This describes the fact that the person is not moving (standing still) at the beginning of the experiment. In the second part of Experiment 2, the person is moving away from the radar system, which results in increasing values of the TV path delay $\tau'(t)$. Fig. 9 presents the estimated TV radial distance $r(t)$ of the walking person. Here again, it can be clearly seen that the person is not moving at the beginning of the experiment and then walks away from the radar system. We also determine the distance walked by the person by computing the difference between $r(t_2)$ and $r(t_1)$, where t_1 =2.5 s (beginning of the walking activity) and t_2=10 s (end of the walking activity). Here, the walking distance is approximately 12 m, which is in accordance with the specifics of the scenario.

VI. Conclusion

In this paper, we estimated the TV path delay and the TV radial distance of a moving person/object in indoor environments from received LFMCW radar signals. The moving

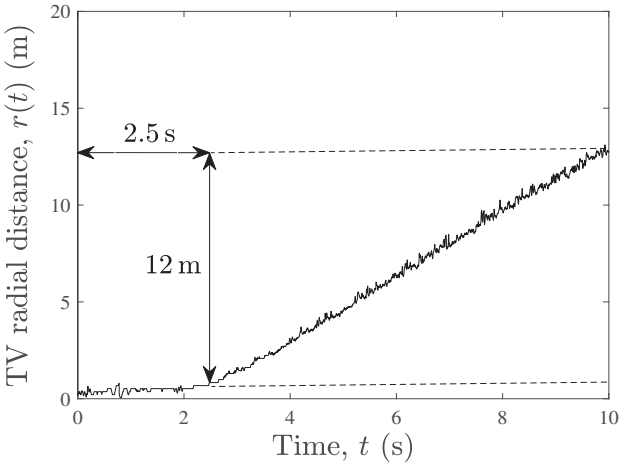

Fig. 9. Estimated TV radial distance $r(t)$ obtained from measurement data for Experiment 2.

person/object is modelled by a single moving point scatterer. By approaching the problem at hand from a channel modelling perspective, the TV range information was extracted from the amplitude of the TV demodulated response of LFMCW radar systems. To validate the proposed technique, we collected RF data using the Ancortek SDR-KIT 2400T2R4 radar system, which operates in the 24 GHz mmWave frequency band. We performed two experiments. In the first one, a pendulum is swinging, and in the second one, a person is walking along a straight line. For the swinging pendulum experiment, a good agreement is observed between the estimated TV radial distance and the corresponding exact quantity. This confirms the validity of the estimation method to track the TV range of a moving person/object in an indoor environment. Since the experiments in this paper were conducted in a controlled indoor environment, the findings of this work can serve as a basis for analysis of the TV range of moving objects in more complex settings. Future work will investigate whether the performance of the proposed estimation algorithm can be improved by using systems with multiple antennas.

Acknowledgment

This work has been carried out within the scope of the CareWell project funded by the Research Council of Norway under the grant number 300638/O70.

References

[1] S. Pisa, E. Pittella, and E. Piuzzi, "A survey of radar systems for medical applications," *IEEE Aero. and Electron. Syst. Mag.*, vol. 31, no. 11, pp. 64–81, Dec. 2016.

[2] N. Ansari, V. K. Sharma, S. Sharma, and V. K. Singh, "Survey on digital signal processing for FMCW radar," in *Emerg. Mater. and Adv. Designs for Wearable Antennas*. IGI Global, 2021, pp. 45–53.

[3] W. G. Carrara, R. S. Goodman, and R. M. Majewski, *Spotlight Synthetic Aperture Radar: Signal Processing Algorithms*. Boston, MA, USA: Artech House, 1995.

[4] A. Tessmann *et al.*, "Compact single-chip W-band FMCW radar modules for commercial high-resolution sensor applications," *IEEE Trans. Microw. Theory and Techn.*, vol. 50, no. 12, pp. 2995–3001, Dec. 2002.

[5] J. Hasch *et al.*, "Millimeter-wave technology for automotive radar sensors in the 77 GHz frequency band," *IEEE Trans. Microw. Theory Techn.*, vol. 60, no. 3, pp. 845–860, Jan. 2012.

[6] A. Rahman *et al.*, "Doppler radar techniques for accurate respiration characterization and subject identification," *IEEE J. Emerg. Sel. Topics Circuits Syst.*, vol. 8, no. 2, pp. 350–359, Jun. 2018.

[7] B. Jin *et al.*, "One-bit LFMCW radar: Spectrum analysis and target detection," *IEEE Trans. Aerosp. and Electron. Syst.*, vol. 56, no. 4, pp. 2732–2750, Mar. 2020.

[8] S. Kim *et al.*, "Signal processing for a multiple-input, multiple-output (MIMO) video synthetic aperture radar (SAR) with beat frequency division frequency-modulated continuous wave (FMCW)," *Remote Sens.*, vol. 9, no. 5, May 2017.

[9] E. Jacobsen and P. Kootsookos, "Fast, accurate frequency estimators [DSP tips & tricks]," *IEEE Signal Process. Mag.*, vol. 24, no. 3, pp. 123–125, 2007.

[10] B. Quinn, "Estimating frequency by interpolation using Fourier coefficients," *IEEE Trans. Signal Process.*, vol. 42, no. 5, pp. 1264–1268, May 1994.

[11] F. Sun, L. Zhu, C. Zhang, and H. Duan, "The research of J-Quinn ranging algorithm for LFMCW radar," in *IEEE Adv. Inf. Manag., Commun., Electron. and Autom. Control Conf. (IMCEC'16)*, Oct. 2016, pp. 1112–1117.

[12] R. Raj, V. Chen, and R. Lipps, "Analysis of radar human gait signatures," *IET Signal Processing*, vol. 4, pp. 234–244, 2010.

[13] A. F. García-Fernández, O. A. Yeste-Ojeda, and J. Grajal, "Facet model of moving targets for ISAR imaging and radar back-scattering simulation," *IEEE Trans. Aero. Electron. Syst.*, vol. 46, no. 3, pp. 1455–1467, 2010.

[14] Z. Zhang *et al.*, "Feature extraction and classification of human motions with LFMCW radar," in *IEEE Int.l Workshop on Electromagnetics: Applications and Student Innovation Competition (iWEM'16)*, Nanjing, China, May 2016, pp. 1–3.

[15] G. Wang *et al.*, "Application of linear-frequency-modulated continuous-wave (LFMCW) radars for tracking of vital signs," *IEEE Trans. Microw. Theory and Techn.*, vol. 62, no. 6, pp. 1387–1399, May 2014.

[16] M. Arsalan, A. Santra, and C. Will, "Improved contactless heartbeat estimation in FMCW radar via Kalman filter tracking," *IEEE Sensors Lett.*, vol. 4, no. 5, pp. 1–4, 2020.

[17] Q. Wu *et al.*, "A non-contact vital signs detection in a multi-channel 77 GHz LFMCW radar system," *IEEE Access*, vol. 9, pp. 49 614–49 628, Mar. 2021.

[18] J. E. Kiriazi, S. M. M. Islam, O. Borić-Lubecke, and V. M. Lubecke, "Sleep posture recognition with a dual-frequency cardiopulmonary Doppler radar," *IEEE Access*, vol. 9, pp. 36 181–36 194, Feb. 2021.

[19] R. Hicheri, N. Avazov, M. Muaaz, and M. Pätzold, "The transfer function of non-stationary indoor channels and its relationship to system functions of LFMCW radars," in *22nd IEEE Int. Workshop on Signal Process. Advances in Wireless Commun. (SPAWC'21)*, Lucca, Italy, Sept. 2021.

[20] R. S. A. R. Abdullah *et al.*, "Micro-Doppler estimation and analysis of slow moving objects in forward scattering radar system," *Remote Sens.*, vol. 9, no. 7, p. 699, Jul. 2017.

[21] S. Kamrul Islam and M. R. Haider, *Sensors and Low Power Signal Processing*. Springer Science & Business Media, 2010.

[22] M. Pätzold, *Mobile Radio Channels*. John Wiley & Sons, 2011.

[23] L. Jing, Z. Yanping, and Z. Xingang, "On the maximum unambiguous range of LFMCW radar," in *Int. Conf. on Inf. Technol. and Comput. Appl. (ITCA'19)*, Guangzhou, China, Dec. 2019, pp. 92–94.

[24] N. Avazov, R. Hicheri, and M. Pätzold, "A trajectory-driven SIMO mm-Wave channel model for a moving point scatterer," in *15th European Conf. on Antennas and Propag. (EuCAP'21)*, Dusseldorf, Germany, Mar. 2021, pp. 1–5.